

s-d* Exchange Interaction in Amorphous Cr-Pd-Si and Mn-Pd-Si Alloys

R. Hasegawa and C. C. Tsuei

W. M. Keck Laboratory of Engineering Materials, California Institute of Technology, Pasadena, California 91109

(Received 5 February 1969; revised manuscript received 26 January 1970)

The electrical and magnetic properties of amorphous alloys obtained by rapid quenching from the liquid state have been studied. The compositions of these alloys are $\text{Cr}_x\text{Pd}_{80-x}\text{Si}_{20}$ and $\text{Mn}_x\text{Pd}_{80-x}\text{Si}_{20}$, in which x is the atomic concentration and ranges between 0 and 7. A well-defined minimum in the resistivity versus temperature is observed for these alloys except for the case where $x=0$. Below the resistivity-minimum temperature T_m , the resistivity difference $\Delta\rho$ varies as $-\ln T$ in agreement with Kondo's theory, and tends to level off at lower temperatures. The resistivity-minimum phenomenon persists in amorphous alloys containing as much as 7 at. % or more of transition metals like Cr or Mn. Also, the resistivity-minimum temperature for some of the amorphous alloys studied can be as high as 580°K. The resistivity-minimum anomaly is always accompanied by a negative magneto-resistivity approximately proportional to the square of the magnetization and a susceptibility obeying the Curie-Weiss law for a wide temperature range. These observations lead to the conclusion that a Kondo-type *s-d* exchange interaction exists in the amorphous Pd-Si alloys containing Cr or Mn. In terms of the *s-d* exchange model, the following statements can be made: (a) The results of susceptibility and magnetoresistivity measurements suggest that the *d-d* spin correlation between magnetic atoms is, in general, weaker in the amorphous alloys than in the corresponding crystalline alloys. This is consistent with the fact that a Kondo-type resistivity anomaly has been observed in amorphous alloys containing 7 at. % Cr or Mn. (b) The spin-compensated state has been observed in the amorphous alloys containing Cr. From the resistivity data, it is concluded that the Kondo temperature of these alloys depends linearly on the Cr concentration. For the Mn-Pd-Si alloys, the spin-compensated state is masked by the *d-d* spin correlation. (c) The *s-d* exchange integrals for the Cr and Mn amorphous alloys are estimated and found to be consistent with Friedel's virtual-bound-state model.

I. INTRODUCTION

Ever since the advent of Kondo's theory¹ to explain the resistivity-minimum phenomenon, the problem of an exchange interaction between conduction electrons and localized moments has been of considerable interest. Many have contributed to the present theoretical understanding of the problem of the *s-d* exchange interaction. A recent review article by Kondo² summarizes theoretical progress concerning this problem. A common feature shared by all these theories is that the effect of correlation between localized spins of impurities on the Kondo effect has not been adequately treated. On the experimental side, the results are in general consistent with the theoretical predictions.³ There remains, however, some uncertainty in understanding the nature of the ground-state conduction-electron spins polarized in the vicinity of a magnetic spin. The reported value of the coherence length varies from 9 \AA^4 to the order of 10^3 \AA .⁵ Furthermore, the previously observed anomalous low-field susceptibility⁶ in Cu-Fe alloys might be explained⁷ in terms of superparamagnetism of small clusters of precipitated Fe atoms. This implies that the spatial distribution of magnetic impurity atoms in a so-called "dilute alloy" may not be as homogeneous as is generally realized. In view of these experimental

findings, the hypothesis of isolated magnetic spins, on which most of the theories and experimental studies have been based, may not be an accurate description of the real situation except in the case of extreme dilution. Thus a systematic study of the Kondo effect in alloys with wide concentration ranges should yield some information about the validity of the isolated-spin assumption.

In this paper, a study of Kondo-type *s-d* exchange interaction in noncrystalline alloys containing transition metals is presented. There are several reasons for the choice of this approach. First, the results of Kondo's theory are applicable to amorphous materials, since the theory does not require a crystal structure. Second, the absence of long-range order in amorphous materials probably reduces the *d-d* spin interaction between magnetic atoms,⁸ which is favorable in the light of the model of isolated magnetic spins. Therefore, amorphous materials offer some advantages over crystalline ones to test the validity of theoretical predictions. Third, it is hoped that the present study can add more insight about the physics of amorphous materials which are of current interest and not well understood.

The palladium-silicon amorphous alloys were chosen for this investigation because in these alloys it is possible to replace Pd by an apprecia-

ble amount of another transition metal. In addition, the structure and the properties of the amorphous $\text{Pd}_{80}\text{Si}_{20}$ alloy have been studied.⁹ In this paper a more complete study¹⁰ is presented on the resistivity, magnetoresistivity, and magnetic susceptibility of the amorphous $\text{Pd}_{80}\text{Si}_{20}$, $\text{Cr}_x\text{Pd}_{80-x}\text{Si}_{20}$, and $\text{Mn}_x\text{Pd}_{80-x}\text{Si}_{20}$ alloys. The data are analyzed in terms of the existing theories on the *s-d* exchange interaction and the results are compared with those found in crystalline alloys containing Cr or Mn. The results for the amorphous Fe-Pd-Si and Co-Pd-Si alloys, where coexistence of Kondo effect and ferromagnetism was found, will be presented later.

II. EXPERIMENTAL METHODS

All the amorphous alloys used in this study were prepared by a rapid quenching technique and specimens were chosen with care from among several quenched foils as described in an earlier paper.¹⁰ The compositions of these alloys are $\text{Cr}_x\text{Pd}_{80-x}\text{Si}_{20}$ and $\text{Mn}_x\text{Pd}_{80-x}\text{Si}_{20}$, in which *x* is the atomic concentration.¹¹ The concentration range within which an amorphous structure could be obtained was 0–7 for Cr and Mn. The purity for the transition metals and for Si were 99.99 and 99.999%, respectively. The resistivity of the amorphous alloys was measured by the four-probe method in the temperature range from 1.5–600 °K. The temperature was measured with an accuracy of better than ± 0.2 °K by a combination of a copper-constantan thermocouple and germanium crystal thermometer. The results of the resistivity measurements are accurate to ± 0.01 $\mu\Omega$ cm, excluding the uncertainty (about 15%) in the dimensions of the specimens. The specimens used in the magnetoresistivity measurements were the same as those used in the resistivity measurements. The transverse magnetoresistivity was measured at 4.2, 77, and 295 °K with the magnetic field varied from 0 to 10 kOe. A Princeton Applied Research model Tc-100.2 BR voltage/current reference source was used in the resistivity and magnetoresistivity measurements with a Leeds and Northrup guarded potentiometer. The magnetic susceptibility of the amorphous alloys was measured between 1.8 and 300 °K and in a magnetic field up to 8.40 kOe. The measurements were made in the null-coil pendulum magnetometer whose design and performance were described elsewhere.¹² The magnetometer was calibrated with a piece of spectrographically pure nickel supplied by Johnson, Matthey and Co., Ltd. and by use of the results given in Ref. 13. The calibration was verified by comparison of the measured susceptibility of pure $\text{HgCo}(\text{SCN})_4$ with the reported values.¹⁴ The ultimate sensitivity of the magnetometer is

4×10^{-6} emu with a field of 8.40 kOe.

III. RESULTS AND DISCUSSIONS

A. Amorphous $\text{Pd}_{80}\text{Si}_{20}$ Alloy

1. Electrical Resistivity

Typical resistivity data, shown in Fig. 1, can be expressed by $(86.30 + 2.8 \times 10^{-4} T^2)$ $\mu\Omega$ cm for $10^\circ\text{K} < T < 40^\circ\text{K}$ and $(86.40 + 7.5 \times 10^{-3} T)$ $\mu\Omega$ cm for $T \geq 100^\circ\text{K}$. These data were taken for the alloy with Pd of purity 99.999%. The resistivity-temperature curve for the alloys with 99.99% pure Pd is similar to the one shown in Fig. 1, except for the appearance of a slight minimum at about 10°K . This minimum can be attributed to the presence of Fe impurity (between 50 and 300 ppm) in Pd. The temperature dependence of the resistivity for different samples varies slightly from that of Fig. 1 due to the uncertainty in the dimensions of the samples.

2. Magnetic Susceptibility

The susceptibility of the $\text{Pd}_{80}\text{Si}_{20}$ alloy was found to be negligibly small ($\chi = 10^{-7} \sim 10^{-8}$ emu/g) between 20 and 300 °K and increases as $1.4 \times 10^{-5} T^{-1}$ emu/g for $T < 20^\circ\text{K}$. The susceptibility enhancement below 20°K is considered to be due to Fe impurities. Assuming the effective magnetic moment of about $5.7 \mu_B/(\text{Fe atom})$,¹⁵ the Fe impurity is estimated as ~ 0.03 at. %.

3. Magnetoresistivity

It was found that the $\text{Pd}_{80}\text{Si}_{20}$ alloy exhibits no observable magnetoresistivity at $T = 77$ and 295°K and a very small positive magnetoresistivity ($\Delta\rho_H = 10 \text{ kOe}/\rho_{H=0} \sim 0.0025\%$) at $T = 4.2^\circ\text{K}$. The Hall coefficient of the $\text{Pd}_{80}\text{Si}_{20}$ alloy was found to be independent of temperature.⁹ These observa-

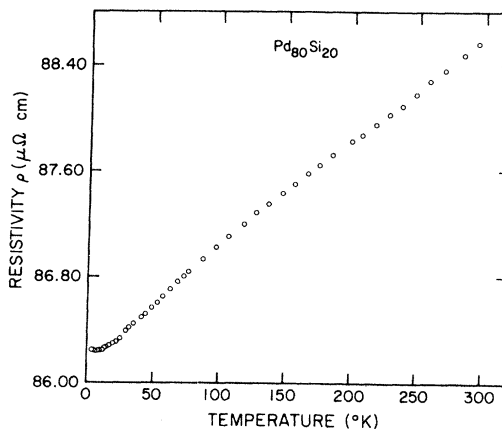


FIG. 1. Electrical resistivity versus temperature for an amorphous $\text{Pd}_{80}\text{Si}_{20}$ alloy.

tions suggest that the nearly-free-electron model can be applied to the amorphous alloy. The general characteristics of the amorphous $\text{Pd}_{80}\text{Si}_{20}$ alloy were found to be quite similar to the amorphous $\text{Ni}_x\text{Pd}_{80-x}\text{Si}_{20}$ ($x = 0$ to 15), $\text{Cu}_x\text{Pd}_{80-x}\text{Si}_{20}$ ($x = 0$ to 5), and $\text{Zn}_x\text{Pd}_{80-x}\text{Si}_{20}$ ($x = 0$ to 3) alloys, in which no localized moment was observed.

B. Chromium in Amorphous Pd-Si Alloys

1. Electrical Resistivity

A well-defined minimum in the resistivity versus temperature was observed for these alloys as shown in Fig. 2. The position of the minimum T_m is plotted as a function of Cr concentration in Fig. 3. The magnetic part of the resistivity is obtained by subtracting the resistivity of the host $\text{Pd}_{80}\text{Si}_{20}$ alloy from that of the $\text{Cr}_x\text{Pd}_{80-x}\text{Si}_{20}$ alloy since Matthiessen's rule is approximately obeyed for the Cr alloys. The temperature variation of the resistivity difference $\Delta\rho (= \rho_{\text{Cr-Pd-Si}} - \rho_{\text{Pd-Si}})$ divided by the resistivity $\Delta\rho(0)$ at the lower-temperature limit is shown in Fig. 4. The most striking result is that the resistivity minimum is observed at relatively high (as high as 580 °K) temperatures and in relatively concentrated alloys

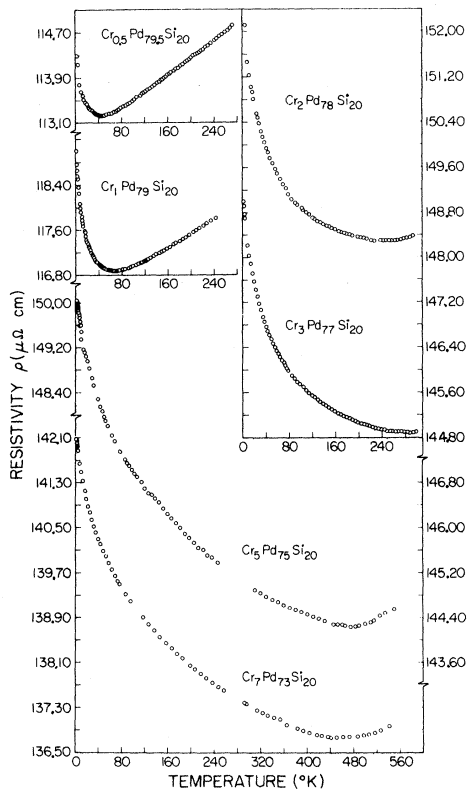


FIG. 2. Electrical resistivity versus temperature for the $\text{Cr}_x\text{Pd}_{80-x}\text{Si}_{20}$ alloys.

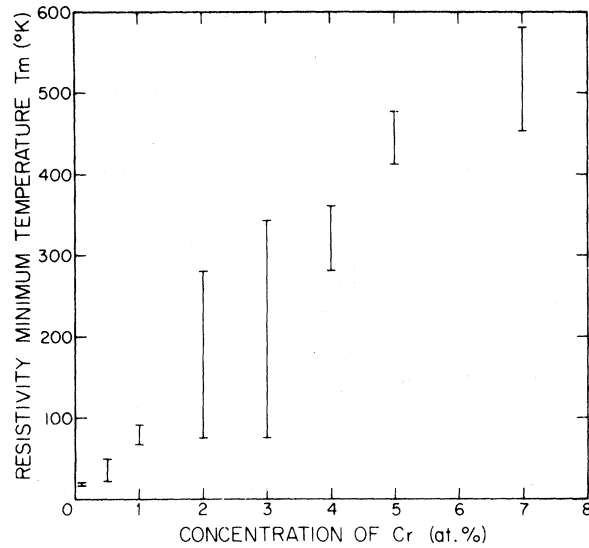


FIG. 3. Resistivity-minimum temperature versus Cr concentration for the $\text{Cr}_x\text{Pd}_{80-x}\text{Si}_{20}$ alloys (taken from Ref. 10).

(up to 7 at. % Cr). It is noticed also that T_m seems to be proportional to Cr concentration and that $\Delta\rho$ generally obeys the logarithmic law of Kondo at higher temperatures and becomes temperature independent at the lower-temperature limit. To interpret these observations, a phenomenological formula for the resistivity for $T > 50$ °K can be written as

$$\rho = \alpha + \beta T + \gamma \ln T, \quad (1)$$

where α represents the temperature-independent part of the resistivity, the second term the non-magnetic temperature-dependent resistivity for $T > 50$ °K, and the third term the spin resistivity due to Kondo.¹ Equation (1) gives a resistivity minimum at

$$T_m = -\gamma/\beta. \quad (2)$$

It is found that β is approximately constant at $7.5 \times 10^{-3} \mu\Omega \text{ cm}$. Typical values of γ are obtained from Fig. 4 and are listed in Table I. Then using Eq. (2) with $\gamma = -0.629x \mu\Omega \text{ cm}$, we find that

$$T_m = 84x(^{\circ}\text{K}) \quad (x \text{ in at. \%}).$$

Thus T_m is proportional to Cr concentration which is consistent with Fig. 3. For $x < 0.5$ (corresponding to $T_m < 50$ °K), we should use a term which is proportional to T^2 instead of βT in Eq. (1). In this case T_m is expected to vary as \sqrt{x} . This is, however, difficult to confirm due to the scattering of T_m data.

Below the resistivity-minimum temperature T_m ,

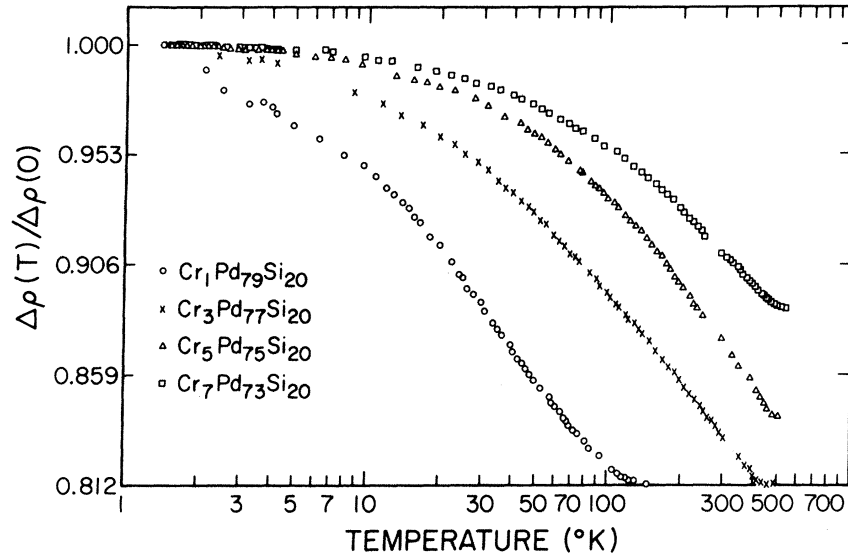


FIG. 4. Resistivity difference per at. % Cr divided by the resistivity $\Delta\rho(0)$ versus temperature for the $\text{Cr}_x\text{Pd}_{80-x}\text{Si}_{20}$ alloys (the data for $\text{Cr}_5\text{Pd}_{75}\text{Si}_{20}$ are taken from Ref. 10).

$\Delta\rho$ obeys the $-\ln T$ law and starts to deviate from it below a characteristic temperature T_d . The temperature T_d depends on Cr concentration and is shown in Fig. 5. Below T_d , $\Delta\rho$ increases more slowly than $-\ln T$, approaching a constant value at lower temperatures. These observations can be explained in terms of the formation of the quasibound state.¹⁶ For this temperature range ($T \ll T_K$), Nagaoka¹⁶ obtained a resistivity formula

$$\Delta\rho = R_0 [1 - (T/T_K)^2], \quad (3)$$

where $R_0 = mx/100 e^2 \pi \hbar N(0)$, m and e being the mass and charge of an electron, \hbar the Planck's constant, and $N(0)$ the density of states of one spin per atom. The Kondo temperature T_K can be expressed by the following formula:

$$T_K \sim D \exp[-1/N(0) |J_{sd}|], \quad (4)$$

where D is the conduction bandwidth and J_{sd} the s - d exchange integral. Using Eq. (3), R_0 and T_K are obtained from the resistivity data at lower temperatures and are listed in Table I. It is noticed that the concentration dependence of T_K is similar to that of T_d , which indicates that the Kondo temperature increases linearly with Cr

TABLE I. Results of the resistivity measurements for the $\text{Cr}_x\text{Pd}_{80-x}\text{Si}_{20}$ alloys.

Alloy composition	γ ($\mu\Omega \text{ cm}$)	R_0 ($\mu\Omega \text{ cm}$)	T_K ($^\circ\text{K}$)
$\text{Cr}_1\text{Pd}_{79}\text{Si}_{20}$	-0.767	22.6	21
$\text{Cr}_3\text{Pd}_{77}\text{Si}_{20}$	-2.17	52.5	76
$\text{Cr}_5\text{Pd}_{75}\text{Si}_{20}$	-3.25	54.7	123
$\text{Cr}_7\text{Pd}_{73}\text{Si}_{20}$	-4.36	46.8	115

concentration. It should be emphasized that this is different from the case of crystalline alloys where T_K is independent of concentration. The apparent increase of T_K with concentration may be attributed to the d - d spin interaction. This is, however, open to speculation.

2. Magnetic Susceptibility

The magnetization of the $\text{Cr}_x\text{Pd}_{80-x}\text{Si}_{20}$ alloys varies linearly with the magnetic field between

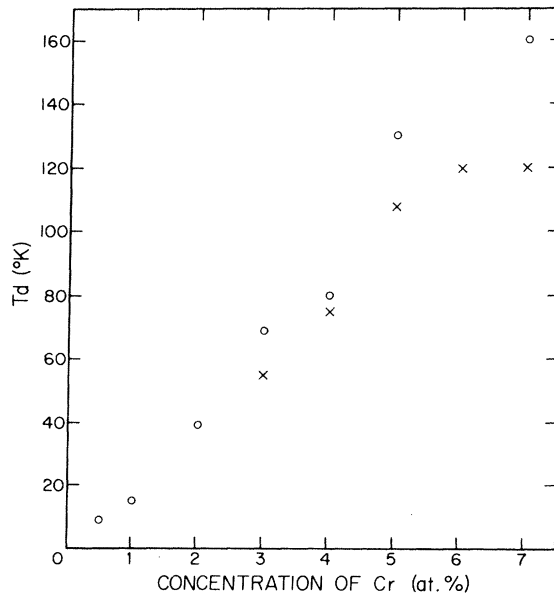


FIG. 5. Temperature at which $\Delta\rho$ deviates from $-\ln T$ law versus Cr concentration for the $\text{Cr}_x\text{Pd}_{80-x}\text{Si}_{20}$ alloys (○). The points (×) are taken from Table II.

1.7 and 300°K, indicating the paramagnetic behavior of the alloys. The magnetization-versus-temperature curves are shown in Fig. 6 for $H = 8.40$ kOe. It is seen that for a given temperature and a given field the magnetization decreases with increasing Cr concentration. At $H = 8.40$ kOe and $T = 4.2$ °K, for example, the magnetization σ_d is found to vary as $\sim 0.24x^{-1} \mu_B/(\text{Cr atom})$ for $2 \leq x \leq 4$. To obtain the contribution of Cr to the observed susceptibility, the difference ($\Delta\chi$) between the susceptibility of the $\text{Cr}_x\text{Pd}_{80-x}\text{Si}_{20}$ alloy and that of the host $\text{Pd}_{80}\text{Si}_{20}$ alloy was studied. The inverse of $\Delta\chi$ is plotted against temperature in Fig. 7, which shows that $\Delta\chi$ obeys the Curie-Weiss law at high temperatures. Thus the results of susceptibility data were analyzed by using the relation

$$\Delta\chi = \mu_{\text{eff}}^2 / 3k(T + \Theta_p) \text{ per atom}, \quad (5)$$

where μ_{eff} is the effective magnetic moment per atom and k the Boltzmann constant. The value of Θ_p may be written¹⁷ as

$$\Theta_p = -S(S+1)J_{dd}x/150k, \quad (6)$$

where S and x are the spin and concentration of the transition metal and J_{dd} is the exchange integral for the d - d spin interaction. The susceptibility difference deviates from the Curie-Weiss law below about 25°K, and undergoes a maximum at $T = T_N$. Above 25°K, curves of $1/\Delta\chi$ versus T seem to consist of two straight lines with a change in slope at the characteristic temperature T_d which depends on Cr concentration (see Fig. 5). As a consequence, the values of μ_{eff} and Θ_p in Eq. (5) are not the same below and above T_d . The results

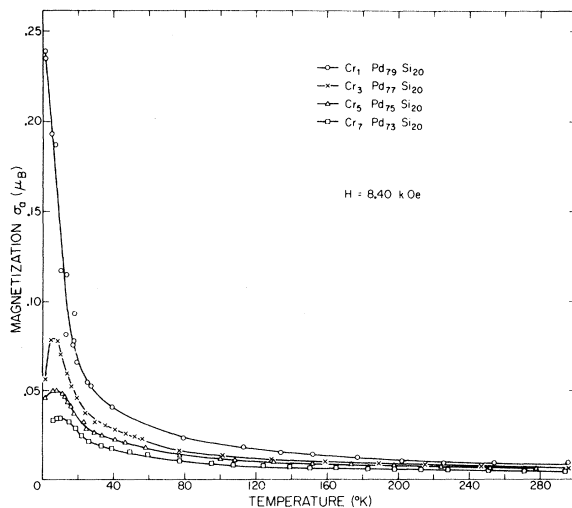


FIG. 6. Magnetization per Cr atom versus temperature at $H = 8.40$ kOe for the $\text{Cr}_x\text{Pd}_{80-x}\text{Si}_{20}$ alloys.

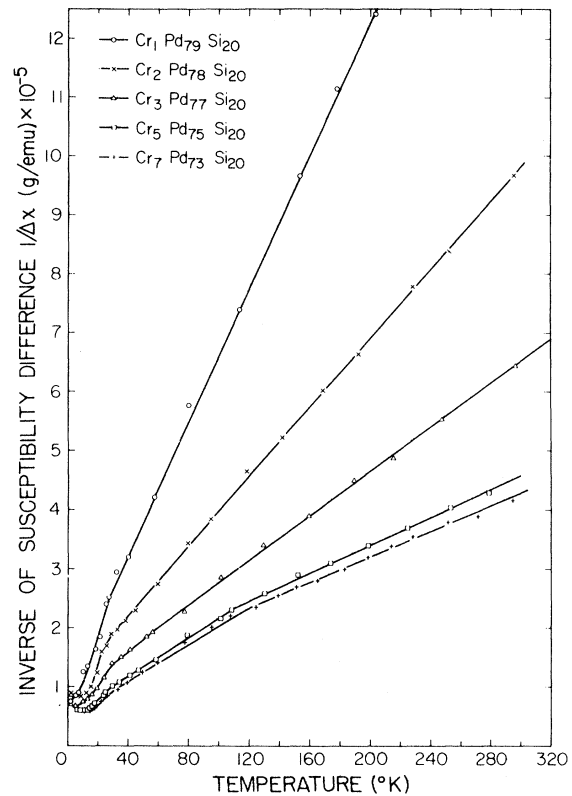


FIG. 7. Inverse of the susceptibility difference per gram of the $\text{Cr}_x\text{Pd}_{80-x}\text{Si}_{20}$ alloys versus temperature (the data for $\text{Cr}_5\text{Pd}_{75}\text{Si}_{20}$ are taken from Ref. 10).

are summarized in Table II. The existing theories¹⁸⁻²³ predict that as T goes to zero the magnetic moment should vanish due to the formation of the quasibound state while the susceptibility becomes finite. This gives another way of writing $\Delta\chi$:

$$\Delta\chi = \mu_{\text{eff}}^2 f(T) / 3kT. \quad (7)$$

The effective magnetic moment $\mu_{\text{eff}}\sqrt{f(T)}$ obtained in this way is shown in Fig. 8. Anderson²⁴ has suggested that for $T \ll T_K$ the value of $\Delta\chi$ would be proportional to $T^{-1/2}$. As shown in Fig. 9, this law seems to be obeyed approximately between T_N and T_d .

The value obtained for μ_{eff} in Table II leads to $S = 2.6/2$ or 2.6 holes in the d shell of Cr. The effective magnetic moment of Cr in crystalline Pd has been measured by Burger²⁵ and is about $4.5 \mu_B/\text{atom}$ which is larger than the present result. The difference between the S value of $\frac{3}{2}$ (assuming Cr^{3+}) and the experimentally determined value of 1.3 suggests that the conduction electrons partly fill the incomplete d shell of Cr. The fact that μ_{eff} is approximately independent of Cr con-

TABLE II. Results of magnetic measurements for the $\text{Cr}_x\text{Pd}_{80-x}\text{Si}_{20}$ alloys.

Alloy composition	$\mu_{\text{eff}} (\mu_B/\text{atom})$ ($T_d < T \leq 300^\circ\text{K}$)	$\Theta_p (^\circ\text{K})$ ($T_d < T \leq 300^\circ\text{K}$)	$\mu'_{\text{eff}} (\mu_B/\text{atom})$ ($25^\circ\text{K} < T < T_d$)	$\Theta'_p (^\circ\text{K})$ ($25^\circ\text{K} < T < T_d$)	$T_N (^\circ\text{K})$	$T_d (^\circ\text{K})$	$\Theta_B (^\circ\text{K})$
$\text{Cr}_1\text{Pd}_{79}\text{Si}_{20}$	3.58	19	3.58	19	< 2	25	16 ~ 24
$\text{Cr}_2\text{Pd}_{78}\text{Si}_{20}$	3.49	35	3.49	35	6	30	25 ~ 44
$\text{Cr}_3\text{Pd}_{77}\text{Si}_{20}$	3.58	50	3.32	36	5	55	42 ~ 56
$\text{Cr}_4\text{Pd}_{76}\text{Si}_{20}$	3.56	67	2.94	30	10	75	54 ~ 74
$\text{Cr}_5\text{Pd}_{75}\text{Si}_{20}$	3.48	80	2.93	32	10	108	67 ~ 109
$\text{Cr}_6\text{Pd}_{74}\text{Si}_{20}$	3.31	90	2.71	35	11	120	93 ~ 120
$\text{Cr}_7\text{Pd}_{73}\text{Si}_{20}$	2.98	91	2.46	28	13	120	102 ~ 127

centration for $T > T_d$ indicates that spin clustering is probably absent in the Cr alloys. The fact that the value of μ'_{eff} for the temperature range between 25°K and T_d is smaller than that above T_d may be due to the formation of the quasibound state. The characteristic temperature T_d is probably the Kondo temperature for the following reasons: (a) T_d is very close to the temperature at which the resistivity difference $\Delta\rho$ deviates from the $-\ln T$ dependence (see Fig. 5). It is also found that T_d is approximately the same as T_K which is obtained from Eq. (3). (b) The effective magnetic moment decreases below T_d as seen in Fig. 8 and Table II. (c) The susceptibility difference $\Delta\chi$ (see Fig. 9) obeys Eq. (7) with a general function

$$f(T) = (0.60 \pm 0.05) (T/T_d)^{1/2}$$

for $T_N < T \ll T_d$. This result gives $\Delta\chi \propto (T/T_d)^{-1/2}$ for $T \ll T_d$ as suggested by Anderson.²⁴ (d) The observed magnetization fits a Brillouin function of the form $B_S[g\mu_B SH/k(T + \Theta_B)]$ with $S = \frac{3}{2}$ and

Θ_B listed in Table II. Since it has been suggested²⁶ that $\Theta_B \sim T_d$ as seen in Table II, it is concluded that $T_K \sim T_d \sim \Theta_B$. The deviation of $\Delta\chi$ from the Curie-Weiss law for $T_N < T < 25^\circ\text{K}$ is probably due to the existence of the quasibound state, since this is the temperature range where $\Delta\chi \propto (T/T_K)^{-1/2}$ holds. The value of $\Delta\chi$ undergoes a maximum at $T = T_N$, below which $\Delta\chi$ decreases very slowly with decreasing temperature. It seems that $\Delta\chi$ approaches a constant value at about 1.3×10^{-5} emu/g or $2.1 \times 10^{-5}/x \mu_B/(\text{Cr atom})$ at the lower-temperature limit. Below T_N , $\mu_{\text{eff}}\sqrt{f(T)}$ decreases rapidly with decreasing temperature, approaching the value of zero moment at absolute zero temperature (see Fig. 8).

The above findings resemble the results of the theoretical predictions that $\Delta\chi$ undergoes the maximum at T_K and approaches a finite value as T goes to zero¹⁸⁻²⁰ and that $\mu_{\text{eff}}\sqrt{f(T)}$ decreases with decreasing temperature below T_K , vanishing at $T = 0^\circ\text{K}$.²¹⁻²³ The present results, however, are

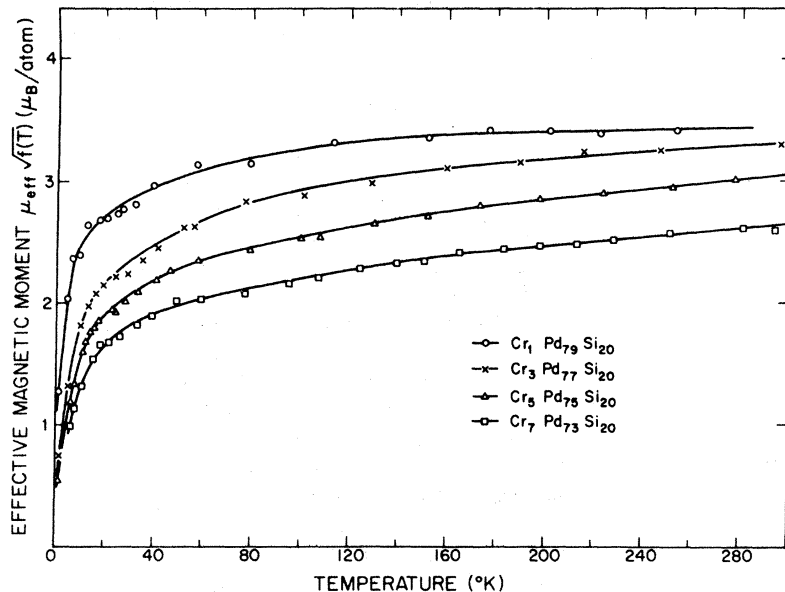


FIG. 8. Effective magnetic moment per Cr atom versus temperature for the $\text{Cr}_x\text{Pd}_{80-x}\text{Si}_{20}$ alloys.

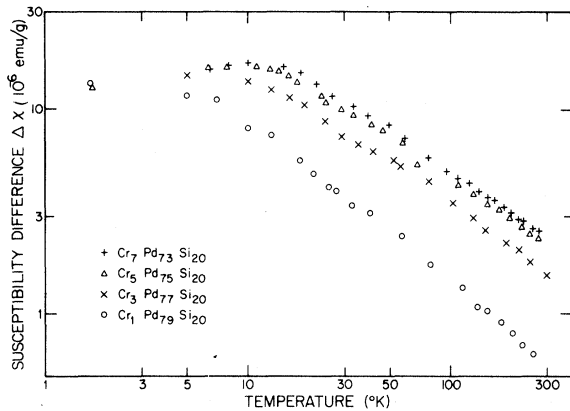


FIG. 9. Susceptibility difference per gram of the $\text{Cr}_x\text{Pd}_{80-x}\text{Si}_{20}$ alloys versus temperature.

probably attributed to the d - d spin interaction, T_N being the antiferromagnetic Néel temperature.

3. Magnetoresistivity

It was found that the $\text{Cr}_x\text{Pd}_{80-x}\text{Si}_{20}$ alloys do not exhibit any observable magnetoresistivity at $T = 77$ and 295 °K but do show an appreciable negative magnetoresistivity at $T = 4.2$ °K. The negative magnetoresistivity $\Delta\rho_H$ is corrected by subtracting the positive magnetoresistivity of $\text{Pd}_{80}\text{Si}_{20}$ from the observed magnetoresistivity and is divided by the resistivity at zero field, $\rho_{H=0}$. The corrected negative magnetoresistivity at $T = 4.2$ °K, shown in Fig. 10, is found to vary as $-b\sigma_a^n$ with b and n

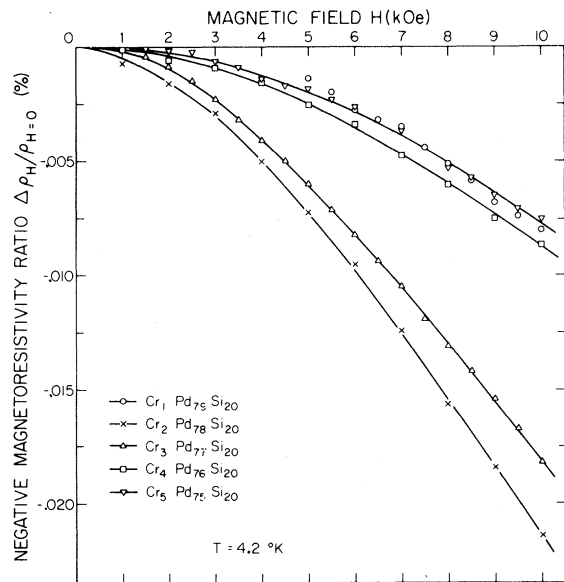


FIG. 10. Negative magnetoresistivity ratio versus magnetic field at 4.2 °K for the $\text{Cr}_x\text{Pd}_{80-x}\text{Si}_{20}$ alloys.

given in Table III. The concentration dependence of the negative magnetoresistivity is shown in Fig. 11 where $\Delta\rho_H = 10 \text{ kOe} / \rho_{H=0}$ is plotted against Cr concentration.

The recent work by Béal-Monod and Weiner²⁷ demonstrates that the negative magnetoresistivity due to the s - d exchange interaction varies as $-b\sigma_a^2$ for $T \gtrsim T_K$. The present result indicates that n is slightly smaller than two. This may be associated with the existence of the quasibound state at 4.2 °K. The absence of a negative magnetoresistivity at 77 and 295 °K may be due to the fact that the magnetization is very small at these temperatures. Two characteristics are noticed in Fig. 11: (i) There is a scattering of $\Delta\rho_H/\rho_{H=0}$ for several alloys with the same concentration of Cr for $x < 4$. (ii) Despite the scattering of the data, it is seen that $|\Delta\rho_H/\rho_{H=0}|$ increases with Cr concentration for $x \leq 2$ and decreases with increasing Cr concentration for $x > 2$. The first characteristic is consistent with the resistivity results since an alloy specimen with a small T_m always has a large negative magnetoresistivity and vice versa. Since the negative magnetoresistivity is proportional to σ_a^2 , some change of σ_a from specimen to specimen would result in an appreciable scattering of $\Delta\rho_H/\rho_{H=0}$. The variation $\Delta\sigma_a$ of σ_a in different specimens with the same nominal composition can be estimated by using the Brillouin function $B_S[g\mu_B SH/k(T + \Theta_B)]$ with $S = \frac{5}{2}$ and with a spread in Θ_B (see Table II). A comparison between the estimated and the experimental error for two specimens is given in Table IV which shows a reasonable agreement. Since $T_m \propto T_K \sim \Theta_B$, it is reasonable to expect that the specimen with a low T_m exhibits a large σ_a resulting in a large negative magnetoresistivity. This clearly explains the correlation between the resistivity and magnetoresistivity data. Thus the scattering of $\Delta\rho_H/\rho_{H=0}$ for a fixed concentration of Cr may indicate that the spatial distribution of σ_a is somewhat different in each specimen.²⁸ The second characteristic of Fig. 11 has been noticed

TABLE III. Typical values of b and n at $T = 4.2$ °K in the expression $\Delta\rho_H/\rho_{H=0} = -b\sigma_a^n$ for the $\text{Cr}_x\text{Pd}_{80-x}\text{Si}_{20}$ alloys.

Alloy composition	b ($\%/\mu_B^2$)	n
$\text{Cr}_1\text{Pd}_{79}\text{Si}_{20}$	0.15	1.89
$\text{Cr}_2\text{Pd}_{78}\text{Si}_{20}$	1.30	1.95
$\text{Cr}_3\text{Pd}_{77}\text{Si}_{20}$	2.25	1.67
$\text{Cr}_4\text{Pd}_{76}\text{Si}_{20}$	1.82	1.80
$\text{Cr}_5\text{Pd}_{75}\text{Si}_{20}$	2.50	1.88
$\text{Cr}_6\text{Pd}_{74}\text{Si}_{20}$	3.61	1.65
$\text{Cr}_7\text{Pd}_{73}\text{Si}_{20}$	4.66	1.53

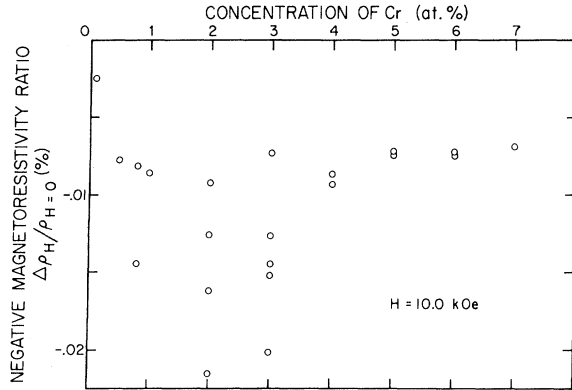


FIG. 11. Negative magnetoresistivity ratio versus Cr concentration at $H = 10.0$ kOe and $T = 4.2$ °K for the $\text{Cr}_x\text{Pd}_{80-x}\text{Si}_{20}$ alloys.

in crystalline alloys.²⁹ The concentration dependence of $\Delta\rho_H/\rho_{H=0}$ for $x > 2$ can be explained from the magnetization data. As mentioned before the magnetization σ_a is inversely proportional to the concentration of Cr for $x > 2$. Then the relation $\Delta\rho_H \propto x\sigma_a^2$ gives $\Delta\rho_H/\rho_{H=0} \propto x^{-1}$ for $x > 2$, as is observed in the Cr alloys. There is a maximum in the $|\Delta\rho_H/\rho_{H=0}|$ versus Cr concentration at $x \sim 2$ (see Fig. 11) when $T = 4.2$ °K and $H = 10.0$ kOe, which is compared with $x \sim 0.1$ for crystalline alloys.²⁹ This fact may indicate that the d - d spin interaction between Cr atoms is weaker in amorphous alloys than in crystalline alloys.

4. s - d Exchange Integral and Localized States for Cr

It may not be justified to determine the s - d exchange integral J_{sd} by applying the result of Béal-Monod and Weiner²⁷ to the magnetoresistivity data (taken at 4.2 °K), since the quasibound state seems to be already formed at 4.2 °K. Equation (3) could be used to find the value for J_{sd} if the density of states were known. The most appropriate method for the present case is probably to use the result of Kondo which gives

$$\gamma = 3p\alpha J_{sd}\rho_M/100E_F, \quad (8)$$

where

Alloy composition	$(\Delta\sigma_a/\sigma_a)_{H=10 \text{ kOe}}$	$\Delta(\Delta\rho_{H=10 \text{ kOe}}/\rho_{H=0})_{\text{est}}$	$\Delta(\Delta\rho_{H=10 \text{ kOe}}/\rho_{H=0})_{\text{expt}}$
$\text{Cr}_2\text{Pd}_{78}\text{Si}_{20}$	$\pm 17\%$	$\pm 34\%$	$\pm 40\%$
$\text{Cr}_6\text{Pd}_{74}\text{Si}_{20}$	$\pm 5\%$	$\pm 10\%$	$\pm 3\%$

$$\rho_M = 3\pi m J_{sd}^2 S(S+1)/2e^2 \hbar n E_F,$$

where p is the number of electrons per atom, n the number of atoms per unit volume, and E_F the Fermi energy. The value of E_F is first evaluated by comparing the experimental and the calculated residual resistivity. Blandin and Friedel¹⁷ have obtained the residual resistivity per at. % (in atomic units):

$$\rho_0 = \frac{2\pi}{pk_F} \sum_l l [\sin^2(\eta_{l-1}^+ - \eta_l^+) + \sin^2(\eta_{l-1}^- - \eta_l^-)], \quad (9)$$

where k_F is the Fermi wave number and the arrows show the direction of the spins in the d shell. The phase shift $\eta_l(E_F)$ can be obtained from the Friedel sum rule³⁰

$$\frac{1}{\pi} \sum_l (2l+1) \eta_l(E_F) = Z, \quad (10)$$

where Z is the number of d electrons having energies below the Fermi level in one of the split d states. The value of η_2 is considered to be the largest since $l=2$ for d states. It can be assumed therefore that $\eta_0, \eta_1, \ll \eta_2$ and $\eta_l = 0$ for $l > 2$. The susceptibility results give $\eta_2^+ \sim \pi/2$ and $\eta_2^- \sim 0$. Thus assuming the free-electron model, E_F is evaluated as 3.5 eV through Eq. (9) with the experimental residual resistivity obtained for alloys with a small concentration (i. e., $\rho_0 \sim 22 \mu\Omega \text{ cm}$). Then from $\gamma = -0.629 \mu\Omega \text{ cm/at. \%}$ (Table I) and $S = 2.6/2$, the value for J_{sd} can be evaluated as -0.76 eV.³¹ This value is compared with -1.4 eV for the crystalline Cr-Zn alloys³² and also with -0.35 eV for the crystalline Cr-Pd alloys.³³ The large value of J_{sd} for the Cr-Pd-Si amorphous alloys is probably responsible for the large resistivity minimum observed. The fact that $S = 2.6/2$ implies that one of the split d states for Cr has its center at the Fermi level in the Friedel model,³⁰ as shown in Fig. 12. These results suggest

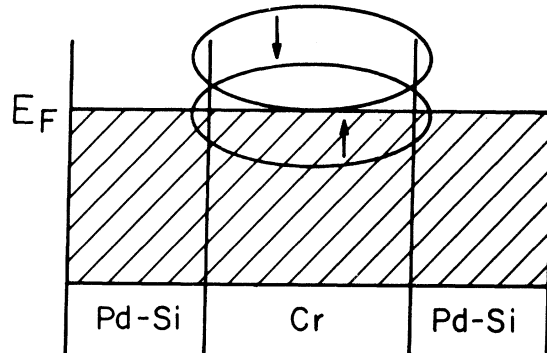


FIG. 12. Friedel's model for the localized d states of Cr in the $\text{Cr}_x\text{Pd}_{80-x}\text{Si}_{20}$ alloys. The arrow shows the direction of the spins in the d states.

that the value of J_{sd} is the largest when S is close to $2.5/2$.

C. Manganese in Amorphous Pd-Si Alloys

1. Electrical Resistivity

Typical resistivity-versus-temperature curves for Pd-Si alloys are shown in Fig. 13. Two characteristics are noticed in this figure: (a) Matthiessen's rule is not satisfied, since the resistivity-temperature coefficient β at higher temperatures changes with Mn concentration. It was found that β is approximately proportional to the inverse of Mn concentration. (b) The resistivity-minimum temperature T_m increases with Mn concentration, which is shown in Fig. 14. Since Matthiessen's rule is not obeyed for these alloys, a simple subtraction of the resistivity of the host $\text{Pd}_{80}\text{Si}_{20}$ alloy from that of the $\text{Mn}_x\text{Pd}_{80-x}\text{Si}_{20}$ alloy does not give a meaningful result. Therefore, it is assumed here that the magnetic part of the resistivity is temperature dependent below T_m while it is constant above T_m . It is further assumed that the nonmagnetic part of the resistivity can be taken as an extrapolation of the resistivity at higher temperatures obeying a T^2 function, to lower temperatures, since the resistivity for the alloys containing lower concentration of Mn varies as T^2 between T_m and about 50°K . Thus the magnetic part of the resistivity is determined as a difference ($\Delta\rho$) between the

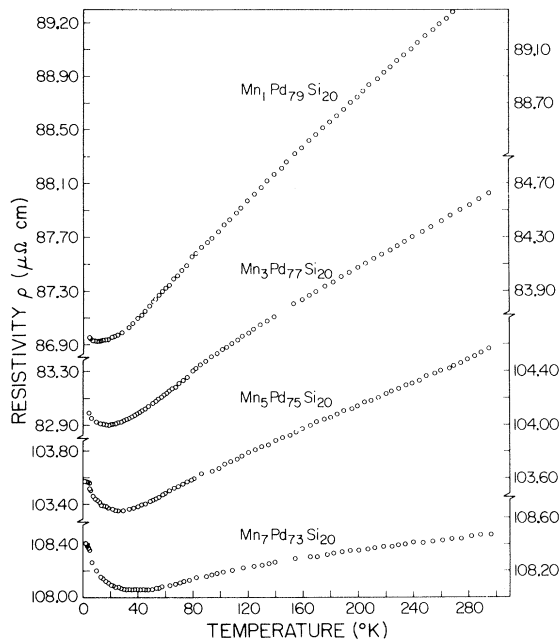


FIG. 13. Electrical resistivity versus temperature for the $\text{Mn}_x\text{Pd}_{80-x}\text{Si}_{20}$ alloys.

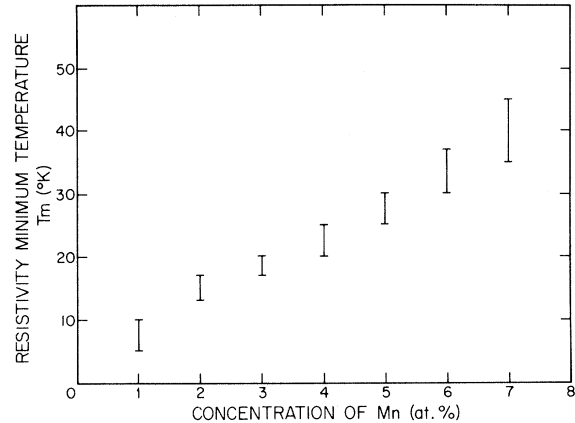


FIG. 14. Resistivity-minimum temperature versus Mn concentration for the $\text{Mn}_x\text{Pd}_{80-x}\text{Si}_{20}$ alloys (taken from Ref. 10).

measured resistivity and the nonmagnetic part defined above, and is shown in Fig. 15 for 3, 5, and 7 at. % Mn. It is noticed in Fig. 15 that the temperature variation of $\Delta\rho$ is independent of Mn concentration and that $\Delta\rho$ varies as $-\ln T$ between $\sim 4^\circ\text{K}$ and T_m and becomes temperature independent below $\sim 4^\circ\text{K}$.

From these data, the resistivity of $\text{Mn}_x\text{Pd}_{80-x}\text{Si}_{20}$ alloys for $T < T_m$ can be described as

$$\rho = \alpha + \delta T^2 + \gamma \ln T, \quad (11)$$

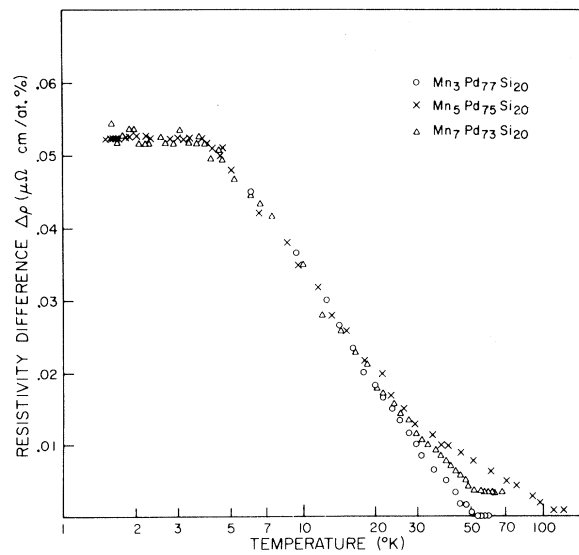


FIG. 15. Resistivity difference per at. % Mn versus temperature for the $\text{Mn}_x\text{Pd}_{80-x}\text{Si}_{20}$ alloys.

where the first and third terms are already mentioned in Eq. (1), the second term being the non-magnetic temperature-dependent part for $T < T_m < 50^\circ\text{K}$. It was found that the coefficient δ is inversely proportional to Mn concentration. The origin of this fact may be the same as that of the concentration dependence of β . Equation (11) gives a resistivity-minimum temperature at

$$T_m = \sqrt{(-\gamma/2\delta)}. \quad (12)$$

From the resistivity data in Figs. 13 and 15, we have $\gamma = -2.3 \times 10^{-2} x \mu\Omega \text{ cm}$ and $x\delta = 2.9 \times 10^{-4} \mu\Omega \text{ cm}$. Then we find that

$$T_m = 6.1x(^{\circ}\text{K}) \text{ for } x < 7 \text{ at.}\%$$

which is in good agreement with the data shown in Fig. 14. The fact that the resistivity difference $\Delta\rho$ levels off below about 4°K suggests the formation of Nagaoka's quasibound states. However, the facts that the temperature variation of $\Delta\rho$ undergoes an abrupt change around 4°K and that $T_N \sim 4^\circ\text{K}$ (see Table V) suggest that the leveling off of $\Delta\rho$ below 4°K is due to the d - d spin correlation between Mn atoms. The Kondo temperature T_K is probably below 4°K for the present case.

2. Magnetic Susceptibility

The results of the magnetic isothermal (magnetization versus magnetic field with temperature as a parameter) for the $\text{Mn}_x\text{Pd}_{80-x}\text{Si}_{20}$ alloys show that the magnetization is proportional to the magnetic field in the temperature range between 1.7 and 300°K , i. e., the alloys behave like paramagnets. The concentration dependence as well as the temperature dependence of the magnetic moments were studied. The magnetization-versus-temperature curves are shown in Fig. 16 for $x = 1, 3, 5,$ and 7 , and for $H = 8.40 \text{ kOe}$. It is found, for example, that the magnetization σ_a varies like $1.15x^{-1/2} (\mu_B/\text{Mn atom})$ for $1 \leq x \leq 5$ and $2.50x^{-1} (\mu_B/\text{Mn atom})$ for $5 \leq x \leq 7$ at $T = 4.2^\circ\text{K}$ and $H = 8.40 \text{ kOe}$. The difference between the susceptibility of the $\text{Mn}_x\text{Pd}_{80-x}\text{Si}_{20}$ and that of the $\text{Pd}_{80}\text{Si}_{20}$ was studied also. The susceptibility difference $\Delta\chi$ obeys the Curie-Weiss law in a temperature range from 4 to 300°K as shown in Fig. 17. The susceptibility data were analyzed through Eq. (5),

TABLE V. Results of magnetic measurements for the $\text{Mn}_x\text{Pd}_{80-x}\text{Si}_{20}$ alloys.

Alloy composition	μ_{eff} (μ_B/atom)	Θ_p ($^\circ\text{K}$)	T_N ($^\circ\text{K}$)	Θ_B ($^\circ\text{K}$)
	$T_N < T < 300^\circ\text{K}$	$T_N < T < 300^\circ\text{K}$		
$\text{Mn}_1\text{Pd}_{79}\text{Si}_{20}$	5.84	1	2	1.0 ± 0.3
$\text{Mn}_3\text{Pd}_{77}\text{Si}_{20}$	5.73	4	4	4.2 ± 0.4
$\text{Mn}_5\text{Pd}_{75}\text{Si}_{20}$	5.56	9	4	7.5 ± 1
$\text{Mn}_7\text{Pd}_{73}\text{Si}_{20}$	5.76	12	4	12.5 ± 1

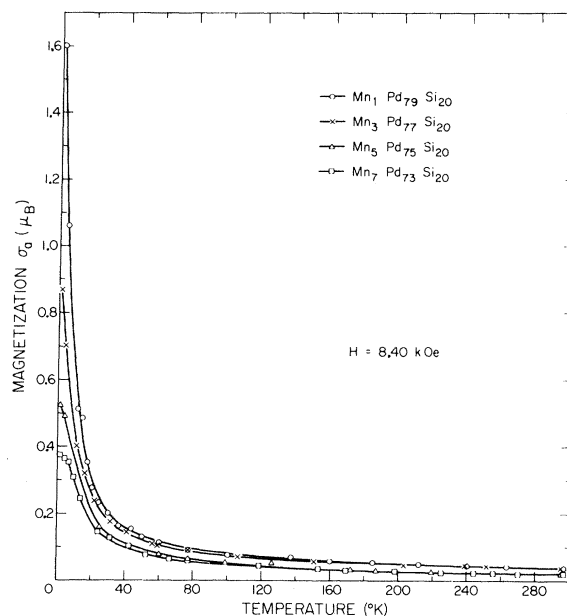


FIG. 16. Magnetization per Mn atom versus temperature at $H = 8.40 \text{ kOe}$ for the $\text{Mn}_x\text{Pd}_{80-x}\text{Si}_{20}$ alloys.

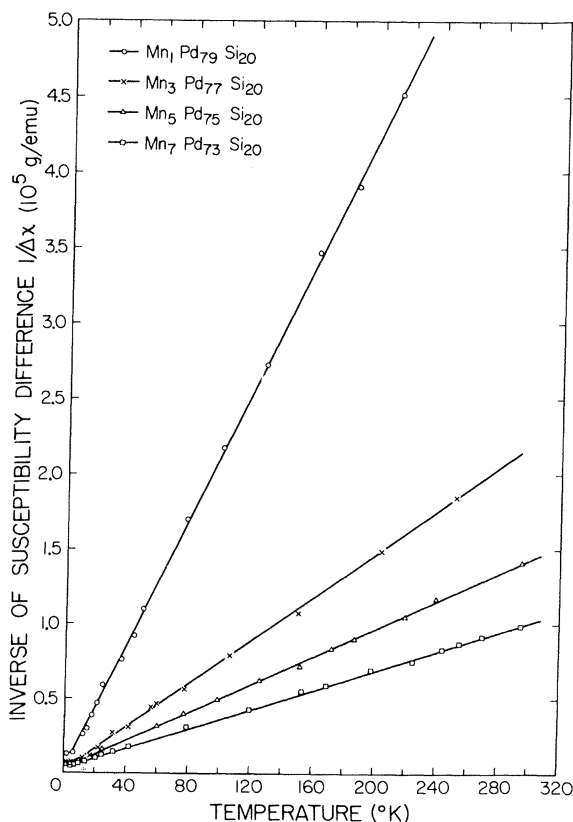


FIG. 17. Inverse of the susceptibility difference per gram of the $\text{Mn}_x\text{Pd}_{80-x}\text{Si}_{20}$ alloys versus temperature.

and the results are summarized in Table V. The results obtained by using Eq. (7) are plotted in Fig. 18.

The invariance of the effective magnetic moment μ_{eff} with respect to Mn concentration suggests that the Mn atoms do not form clustering. The observed value for μ_{eff} gives $S = 4.9/2$ or 4.9 holes per Mn atom and this indicates that the Mn atom behaves as Mn^{2+} ion in the alloy. The fact that S is very close to $\frac{5}{2}$ shows that the d shell of the Mn atom is hardly filled with the conduction electrons. Burger²⁵ has obtained $S \sim \frac{5}{2}$ for Mn in crystalline Pd, which indicates that the electronic structure of Mn is not very much altered by the presence of Pd atoms. The situation may be the same in the present alloys. It is found also that $\Theta_p/\text{at.}\%$ Mn for the amorphous Mn-Pd-Si alloys is about 1.2°K which is smaller than that for the crystalline Mn-Pd alloys ($\sim 4.5^\circ\text{K}$).²⁵ This implies that the d - d spin correlation is weaker in the amorphous alloys than in the crystalline alloys. This is quite favorable for the s - d exchange interaction since the d - d spin correlation tends to reduce the effect of the s - d interaction.³⁴ The magnetic moments observed in the Mn alloys can be expressed by a Brillouin function of the form $B_S[g\mu_B SH/k(T + \Theta_B)]$ with $S = \frac{5}{2}$ and Θ_B listed in Table V. It is noticed that $\Theta_B \sim \Theta_p$, which is to be expected since the Curie-Weiss law holds between 4 and 300°K . The susceptibility difference $\Delta\chi$ has a maximum at T_N and then decreases with decreasing temperature. The value of $\mu_{\text{eff}}\sqrt{f(T)}$ decreases rapidly below T_N as seen in Fig. 18. These findings can be interpreted as a result of the d - d spin interaction between Mn atoms as in the case of the amorphous Cr-Pd-Si alloys. Thus, T_N is considered as the antiferromagnetic transition temperature for the

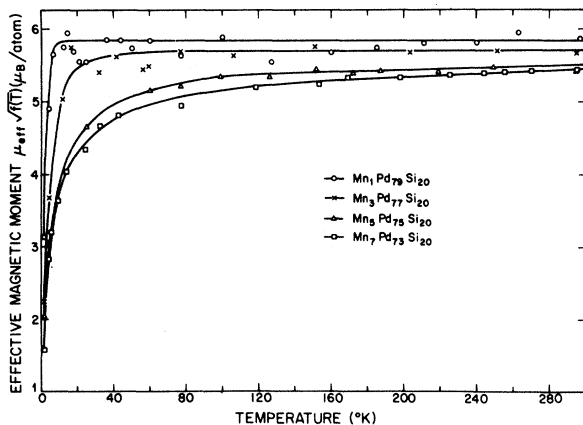


FIG. 18. Effective magnetic moment per Mn atom versus temperature for the $\text{Mn}_x\text{Pd}_{80-x}\text{Si}_{20}$ alloys.

present alloys.

3. Magnetoresistivity

No magnetoresistivity was observed at $T = 77$ and 295°K for $\text{Mn}_x\text{Pd}_{80-x}\text{Si}_{20}$ alloys. An appreciable negative magnetoresistivity was obtained at $T = 4.2^\circ\text{K}$. The negative magnetoresistivity $\Delta\rho_H$ is corrected similarly to the case of Cr-Pd-Si alloys, and the curves for $\Delta\rho_H/\rho_{H=0}$ at $T = 4.2^\circ\text{K}$ are shown in Fig. 19 for Mn concentrations of 1, 3, 5, and 7 at.%. The absence of a negative magnetoresistivity at $T = 77$ and 295°K is probably due to a small value of σ_a at these temperatures (see Fig. 16). The results of the negative magnetoresistivity can be fitted to the general function $\Delta\rho_H/\rho_{H=0} = -b\sigma_a^n$ with b and n given in Table VI. The fact that $n \sim 2$ implies that the quasibound states are not fully formed at 4.2°K . To study the concentration dependence of the negative magnetoresistivity, $\Delta\rho_{H=10\text{ kOe}}/\rho_{H=0}$ at 4.2°K is plotted against Mn concentration in Fig. 20. It is noticed that the absolute value of the negative magnetoresistivity increases with Mn concentration for $x \leq 6$ and decreases for $x > 6$. This characteristic is reasonably consistent with the dependence of σ_a on Mn concentration (see Fig. 16). From Fig. 16 we have $\sigma_a \propto x^{-1/2}$ for $x \leq 5$. Thus we obtain $\Delta\rho_H/\rho_{H=0} \propto -x$ since b varies like x^2 for $x \leq 5$. For $x > 6$, $\Delta\rho_H/\rho_{H=0}$ probably varies like x^{-1} , since $\sigma_a \propto x^{-1}$ for $x > 6$. The striking result is that the concentration at which $|\Delta\rho_H/\rho_{H=0}|$ is a maximum is very large, i. e., about 6 at.% when $T = 4.2^\circ\text{K}$ and $H = 10.0\text{ kOe}$. This is compared with the concentration of the order of less than 0.1 at.% in crystalline alloys,²⁹ in which similar maximum has been observed. These facts again indicate that the d - d spin interaction between transition-metal atoms is weaker in amorphous alloys than in crystalline alloys. The small scattering of the data in Fig. 20 indicates that the magnetization does not vary very much from specimen to specimen. This is confirmed by fitting the magnetization data to the Brillouin function $B_S[g\mu_B SH/k(T + \Theta_B)]$ with $S = \frac{5}{2}$ and Θ_B given in Table V. For example, the estimated error on $\Delta\rho_H/\rho_{H=0}$ due to the error on σ_a is found to be $\pm 6\%$ for the $\text{Mn}_3\text{Pd}_{77}\text{Si}_{20}$ alloy. This error is considerably smaller than those for Cr alloys discussed in Sec. III B.

4. s-d Exchange Integral and Localized States for Mn

By using Eq. (8) with $\gamma = -0.023x \mu\Omega\text{ cm}$ (from Fig. 15), $S = 4.9/2$, and $E_F = 3.5\text{ eV}$, we obtain $J_{sd} \sim -0.18\text{ eV}$ ³¹ for the Mn-Pd-Si alloys. The value of J_{sd} is compared with $J_{sd} = -0.4\text{ eV}$ for a dilute crystalline Cu-Mn alloy³⁵ for which $S = \frac{5}{2}$. A large value of $J_{sd}(-1.4\text{ eV})$ obtained for a dilute crystal-

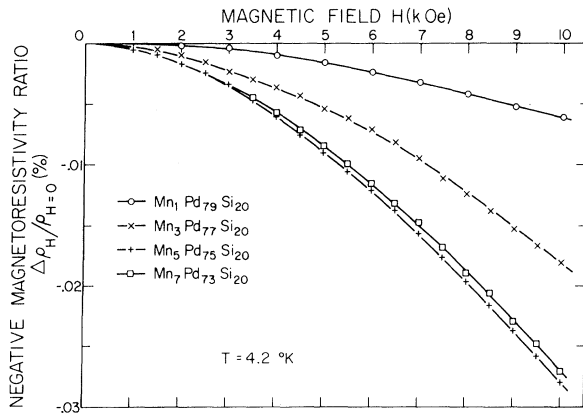


FIG. 19. Negative magnetoresistivity ratio versus magnetic field at 4.2 °K for the $\text{Mn}_x\text{Pd}_{80-x}\text{Si}_{20}$ alloys.

line Zn-Mn alloy³² may be due to the fact that $S = \frac{3}{2}$. In view of Friedel's model,³⁰ one of the split d states for the amorphous Mn-Pd-Si alloys and for the crystalline Cu-Mn alloys is considered to be above and adjacent to the Fermi level while it has its center near the Fermi level for the crystalline Zn-Mn alloys. The case for the Mn-Pd-Si alloys is shown in Fig. 21 and that for the Zn-Mn alloys is probably similar to the Cr-Pd-Si case shown in Fig. 12. This difference may explain the fact that $|J_{sd}|$ for the Mn-Pd-Si and Cu-Mn alloys is smaller than that for the Zn-Mn alloys.

IV. SUMMARY AND CONCLUSIONS

The electrical resistivity, the magnetic susceptibility, and the magnetoresistivity of amorphous palladium-silicon base alloys containing Cr or Mn have been studied. A well-defined minimum in the resistivity-versus-temperature curve is observed in these alloys. Below the resistivity-minimum temperature T_m , the resistivity difference $\Delta\rho$ varies as $-\ln T$ in agreement with Kondo's theory and tends to level off at lower temperatures. It is also found that T_m is linearly proportional to the concentration of Cr and Mn. This is different from the case of crystalline alloys where T_m varies as the $\frac{1}{5}$ power of the transition-metal concentra-

TABLE VI. Values of b and n at $T = 4.2$ °K in the expression $\Delta\rho_H/\rho_{H=0} = -b\sigma_a^n$ for the $\text{Mn}_x\text{Pd}_{80-x}\text{Si}_{20}$ alloys.

Alloy composition	b ($\%/\mu_B^n$)	n
$\text{Mn}_1\text{Pd}_{79}\text{Si}_{20}$	0.0035	2.00
$\text{Mn}_3\text{Pd}_{77}\text{Si}_{20}$	0.0235	2.04
$\text{Mn}_5\text{Pd}_{75}\text{Si}_{20}$	0.0760	1.91
$\text{Mn}_7\text{Pd}_{73}\text{Si}_{20}$	0.110	1.68

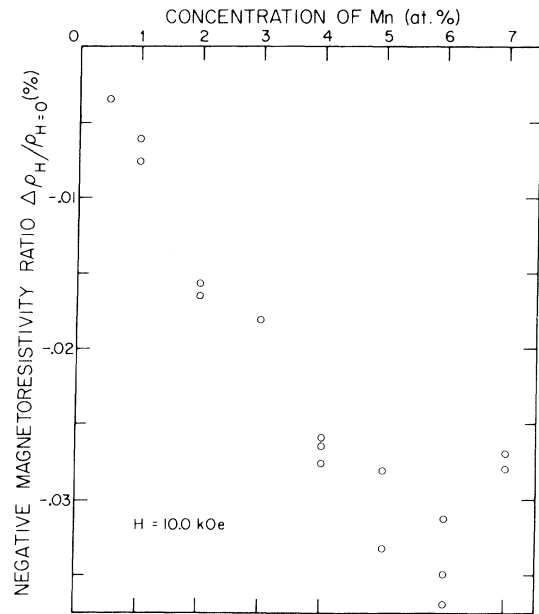


FIG. 20. Negative magnetoresistivity ratio versus Mn concentration at $H = 10.0$ kOe and $T = 4.2$ °K for the $\text{Mn}_x\text{Pd}_{80-x}\text{Si}_{20}$ alloys.

tion. This difference originates from the fact that, in the temperature range where the resistivity minimum occurs, the nonmagnetic part of the resistivity of the amorphous alloys varies as δT^2 (where δ is inversely proportional to Mn concentration) for the Mn alloys and depends linearly on temperature for the Cr alloys. It is interesting to notice that the resistivity-minimum phenomenon persists in amorphous alloys containing as much as 7 at.% or more of transition metals like Cr or Mn. Also, the resistivity-minimum temperature for some of the amorphous alloys studied can be

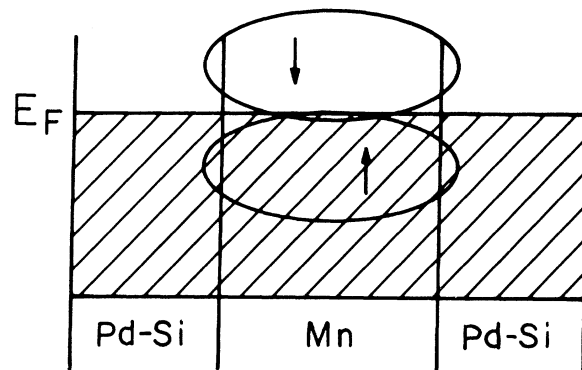


FIG. 21. Localized d states of Mn in the $\text{Mn}_x\text{Pd}_{80-x}\text{Si}_{20}$ alloys in light of Friedel's model.

as high as 580 °K. The resistivity–minimum anomaly is always accompanied by a negative magnetoresistivity approximately proportional to the square of the magnetization and a susceptibility obeying the Curie-Weiss law over a wide temperature range. These observations lead to the conclusion that a Kondo-type *s-d* exchange interaction exists in the amorphous Pd-Si alloys containing Cr or Mn. These results also indicate that the theories based on the isolated-spin assumption are applicable to these nondilute amorphous alloys.

In terms of the *s-d* exchange model, the following statement can be made: (i) The results of the susceptibility and magnetoresistivity measurements suggest that the *d-d* spin correlation between magnetic atoms is, in general, weaker in the amorphous alloys than in the corresponding crystalline alloys. This is consistent with the fact that a Kondo-type resistivity anomaly has been observed in amorphous alloy containing 7 at.% Cr or Mn. (ii) The spin-compensated state has been observed in the amorphous alloys containing Cr.

From the resistivity data it is concluded that the Kondo temperature of these alloys depends linearly on the Cr concentration. This unusual concentration dependence of the Kondo temperature is not well understood. For the Mn-Pd-Si alloys, the spin-compensated state is masked by the *d-d* spin correlation which takes place above the Kondo temperature. (iii) The *s-d* exchange integrals for the Cr and Mn amorphous alloys are estimated and found to be consistent with Friedel's virtual-bound-state model. The results suggest that the value of the *s-d* exchange integral is the largest when the spin of the magnetic atom is close to 2.5/2.

ACKNOWLEDGMENTS

The authors wish to express their sincere gratitude to Professor Pol Duwez for his encouragement and advice during this work. Several communications with Dr. J. Kondo are gratefully appreciated. This work was made possible also through the assistance of R. N. Y. Chan, P. K. Kuan, Y. Moriwaki, and J. E. Brown.

*Work supported by the U. S. Atomic Energy Commission.

¹J. Kondo, *Progr. Theoret. Phys. (Kyoto)* **32**, 37 (1964).

²J. Kondo, *Denki Shikensho Kenkyu Hokoku*, No. 688 (1968).

³M. D. Daybell and W. A. Steyert, *Rev. Mod. Phys.* **40**, 380 (1968).

⁴D. C. Golibersuch and A. J. Heeger, *Solid State Commun.* **8**, 17 (1970).

⁵A. P. Klein, *Phys. Rev.* **181**, 579 (1969).

⁶M. D. Daybell and W. A. Steyert, *Phys. Rev.* **167**, 536 (1968).

⁷D. C. Golibersuch and A. J. Heeger, *Phys. Rev.* **182**, 584 (1969).

⁸R. Hasegawa, *Solid State Phys. (Japan)* **5**, 63 (1970).

⁹R. C. Crewdson, Ph. D. thesis, California Institute of Technology, 1966 (unpublished).

¹⁰A preliminary result of the present study has been reported by C. C. Tsuei and R. Hasegawa, *Solid State Commun.* **7**, 1581 (1969).

¹¹All compositions are stated as atomic percentages.

¹²M. E. Weiner, Ph. D. thesis, California Institute of Technology, 1968 (unpublished).

¹³R. M. Bozorth, *Ferromagnetism* (Van Nostrand, San Francisco, 1951), p. 867.

¹⁴B. N. Figgis and R. S. Nyholm, *J. Chem. Soc.* 4190 (1958).

¹⁵R. Hasegawa, *J. Appl. Phys.* **41**, 4096 (1970).

¹⁶Y. Nagaoka, *Phys. Rev.* **138**, A1112 (1965); *Progr. Theoret. Phys. (Kyoto)* **37**, 13 (1967).

¹⁷A. Blandin and J. Friedel, *J. Phys. Radium* **20**, 160 (1959).

¹⁸K. Yosida and A. Okiji, *Progr. Theoret. Phys. (Kyoto)* **34**, 505 (1965).

¹⁹F. Takano and T. Ogawa, *Progr. Theoret. Phys. (Kyoto)* **35**, 343 (1966).

²⁰A. J. Heeger and M. A. Jensen, *Phys. Rev. Letters* **18**, 488 (1967).

²¹K. Yosida, *Phys. Rev.* **147**, 223 (1966).

²²P. W. Anderson, *J. Appl. Phys.* **37**, 1194 (1966).

²³D. R. Hamann, *Phys. Rev.* **158**, 570 (1967).

²⁴P. W. Anderson, *Phys. Rev.* **164**, 352 (1967).

²⁵J. P. Burger, *J. Phys. Radium* **23**, 530 (1962).

²⁶M. D. Daybell and W. A. Steyert, *Phys. Rev. Letters* **20**, 195 (1968).

²⁷M. T. Béal-Monod and R. A. Weiner, *Phys. Rev.* **170**, 552 (1968).

²⁸This is probably due to the fact that the rate of cooling differs from specimen to specimen prepared by rapid quenching [see P. Duwez, in *Techniques of Metals Research*, edited by R. F. Bunshah (Interscience, New York, 1968), Chap. 7].

²⁹A. N. Gerritsen, *Physica* **19**, 6 (1953).

³⁰J. Friedel, *Can. J. Phys.* **34**, 1190 (1956); *Nuovo Cimento* **7**, 287 (1958).

³¹The value of J_{sd} reported in Ref. 10 was obtained following the analysis used in Ref. 27.

³²G. Boato, G. Gallinaro, and C. Rizzuto, *Phys. Rev.* **148**, 353 (1966).

³³R. Schwaller and J. Wucher, *Compt. Rend.* **116**, 264 (1967).

³⁴This problem was first considered by K. Yosida [*Phys. Rev.* **107**, 396 (1957)]. For some recent works, see A. A. Abrikosov, *Physics* **2**, 61 (1965); S. H. Liu, *Phys. Rev.* **137**, 1209 (1965); S. D. Silverstein, *Phys. Rev. Letters* **16**, 446 (1966); R. J. Harrison and M. W. Klein, *Phys. Rev.* **154**, 540 (1967) or M. T. Béal-Monod, *ibid.* **178**, 874 (1969).

³⁵P. Monod, *Phys. Rev. Letters* **19**, 1113 (1967).